ARMA 16-0027

New Techniques for Monitoring and Analyzing the Stability of Steep Cliffs against Rock Falls

Fujii, Y., Maeda, S., Sugawara, T.
Hokkaido University, Sapporo, Hokkaido, Japan
Kodama, N.
National Institute of Technology, Hakodate College, Hakodate, Hokkaido, Japan
Miyashita, N.
Docon, Sapporo, Hokkaido Japan

ABSTRACT: Mechanisms of joint opening leading to the formation of unstable rock blocks, such as thermal deformation, water-mineral reaction, pore pressure, freeze-thaw cycle, intrusion of wood roots etc. have been more or less clarified; however, the triggering mechanisms of rock falls remain to be elucidated. The problems which prevent the understanding of the mechanisms are (1) difficulty in installation of sensors to very unstable rock blocks, (2) thermoelastic deformation of sensors and attachments, (3) thermoelastic deformation of rock mass and (4) countermeasures to rock falls. Installation of a tiltmeter on the top of a very unstable rock block, correction of thermoelastic deformation of either sensors and attachments or rock mass, and long-term monitoring at a rock cliff along an abandoned road are shown as solutions to the problems. The solutions may not appear to be particularly novel, sophisticated or attractive, but the authors are convinced that they will contribute to breakthroughs in solving the listed problems. The techniques are inexpensive and worth trying.

1. INTRODUCTION

Numerous rock slope-monitoring studies have been conducted, and mechanisms of joint opening leading to the formation of unstable rock blocks, such as thermal deformation, water-mineral reaction, pore pressure, freeze-thaw cycle, intrusion of wood roots etc. have been more or less clarified; however, the triggering mechanisms of rock falls remain to be elucidated.

Problems preventing the advancement of understanding of the mechanisms effecting unstable rock block fall are as follows.

Problem 1: Usually, sensors are connected to rock blocks by anchors and bolts; as such, it has up to date been impossible to install sensors in rock blocks because they are so unstable that they would easily fall during drilling. The monitored rock blocks will never fall because they are stable enough that they can be drilled without falling. Data describing rock fall processes cannot be obtained from such monitoring, and so the mechanisms of rock fall will never be clarified, even if the monitoring is carried out using the latest sensors, which are packed with a range of high-cost technologies.

Problem 2: Measured displacement data, except for tilt data, contain a thermal expansion component attributable to the sensors and attachments. This expansion should be removed from the raw data before interpretation.

Problem 3: Measured data pertains to thermoelastic and inelastic deformation of the rock mass. The thermoelastic deformation component should be removed to extract the inelastic deformation component, which might lead to rock falls.

Problem 4: In most cases, dangerous rock blocks are cut or reinforced so that rock fall is avoided; as such, data during rock fall are rarely obtained.

It is necessary to find solutions to the identified problems rather than spending a large budget on improving the accuracy, and increasing the number, of sensors. Before describing the attempts to solve the identified problems, the basic mechanism of thermal deformation of a rock block is explained.

Next, problems 2–4 are addressed. To address problem 2, a simple technique is presented, which can account for the thermoelastic deformation of displacement sensors and attachments (which thus far has been very difficult), based on the numerical results obtained using the finite element method (FEM), i.e., that a rock block of around 10 m does not deform significantly according to daily temperature variation, but has significant yearly

thermoelastic deformation. To resolve problem 3, a technique similar to the one described above can be used.

To address problem 4, data has been collected at a rock cliff along an abandoned road. Finally, a technique to monitor the deformation of a very unstable rock block is proposed to resolve problem 1.

2. THE BASIC MECHANISMS OF THERMAL DEFORMATION OF ROCK BLOCKS

Rocks shrink with decrease in temperature and expand as temperature rises, as does any other materials except for the phase transition between solid and liquid of water and gallium. Rock surface temperature variations may be caused by insolation, radiation, or the difference in temperature of the surrounding air, surface water flow, rain drops or snow. On the other hand, the temperature deep within the rock mass is, needless to say, almost constant (ex. Mufundirwa et al., 2010). The temperature gradient between the rock surface and the inside rock mass causes thermal stress and thermoelastic deformation and as such is one of the causes of joint opening at a rock cliff face, which may then form unstable rock blocks and potentially lead to rock falls.

Large thermal stresses and thermoelastic deformations can be observed for beam-like rock blocks, as already reported by Negishi & Nakajima (1993) and our reserch group (Keppetipola et al., 2013 and Maeda et al. 2015). For example, in the model analysis of a rock mass with a fracture (Fig. 1, Table 1., Maeda et al., 2015), yearly temperature variation is attributed to the air surrounding the rock mass (Fig. 2). A fracture opening is caused by shrinkage of the outside of the block (Fig. 3a) when the air temperature falls. The fracture closes when air temperature rises, due to the expansion of outside of the rock block (Fig. 3b).

Negishi & Nakajima (1993) considered that the rock block could break at the bottom when the fracture closed if rock fragments were trapped in the fracture. One of the papers by our research group, Keppetipola et al. (2013), showed that the rock block could break when the fracture completely closed even without trapped rock fragments and the reaction force could become particularly large if the rock surface froze and expanded considerably (Fig. 3c).

Table 1. Parameters used in the FE analysis which were measured for rocks sampled at the Toyosaki monitoring site (Fig. 7).

Tangent modulus	94.5 GPa
Poisson's ratio	0.2
Heat conductivity	2.02 W/(mK)
Specific heat	1,183 J/(kg K)
Expansion coefficient	5.88 x 10^{-6} K^{-1}
Density	2,718 kg/m^3
Effective porosity	3.61%
Heat transfer coefficient	3.00 W/(m^2K)

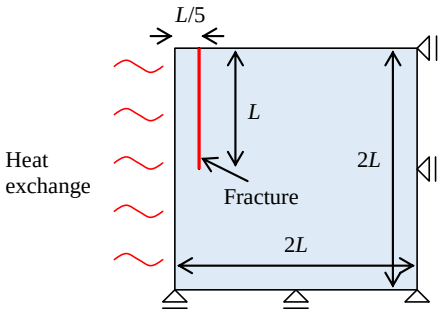

Fig. 1. A rock mass model with a fracture. Right and the bottom boundaries are insulated. The upper boundary was also assumed to be insulated due to vegetation, soil or snow.

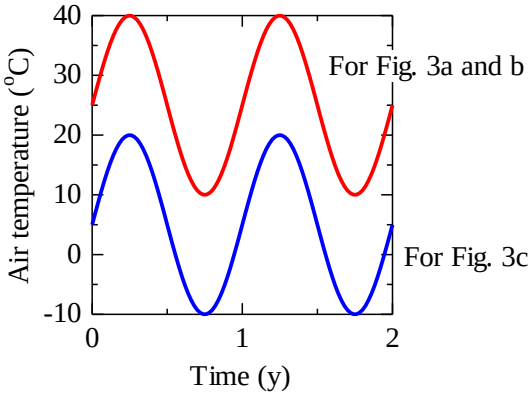

Fig. 2 Two cases of applied air temperature. The colder case is an approximation of the measured result at Toyosaki monitoring site (Fig. 7). The warmer case is to avoid freezing of rock for simplicity.

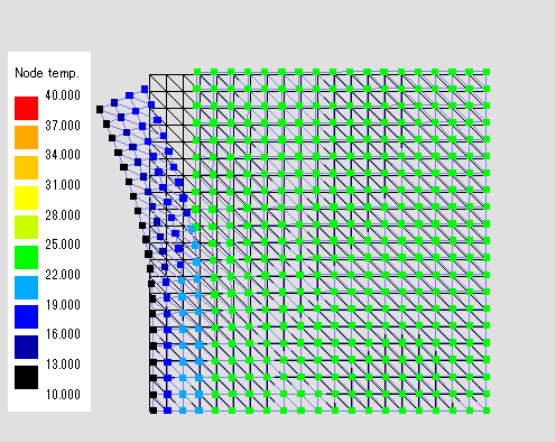

(a) When temperature falls

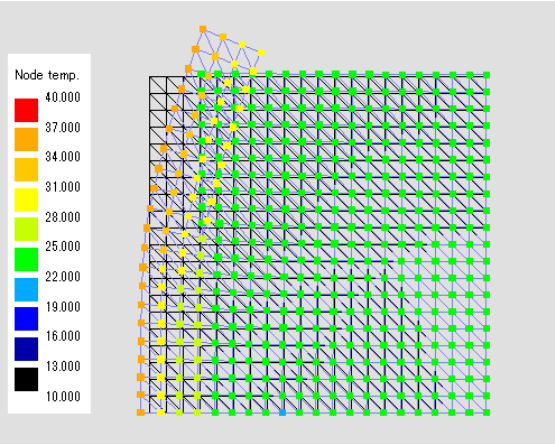

(b) When temperature rises

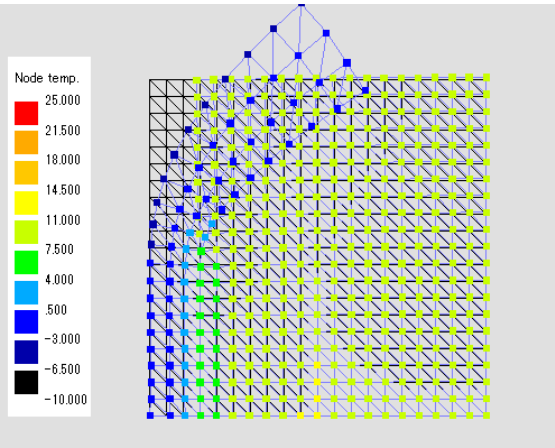

(c) When the rock surface freezes

Fig. 3. Mechanisms of thermal deformation of the rock block shown in Fig. 1 (L = 10 (m), Maeda et al., 2015). Displacement is magnified by 150 times. This model allows fracture closure for simplicity. The temperature at the both sides of the open fracture can be different because the air between the fracture sides insulate the heat transfer. The variation in air temperature is transferred toward inside the rock mass and sometimes show slight temperature disturbances even in the mid of the model (the yellow part at the bottom of (c)).

3. TECHNIQUE TO CORRECT THE THERMAL DEFORMATION OF A DISPLACEMENT SENSOR AND THE ATTACHMENT

FE analyses for the model shown in Fig. 1 were carried out varying the period of temperature variation for the warmer case (Fig. 2). The results (Fig. 4) showed that thermoelastic deformation of rock mass was smaller when the rate of change in temperature was very fast or slow. This is because heat does not conduct to inside of rock mass when the variation is too fast (Fig. 5a) and the temperature distribution approaches uniform when the variation is slow (Fig. 5c). Typically, daily temperature change is too fast and does not cause rock mass thermoelasic deformation (Fig. 5a). On the other hand, seasonal variation causes seasonal large deformation (Fig. 5b). Measured daily variation in displacement is therefore mainly due to thermoelastic deformation of the sensors and the attachments.

Let's assume the seasonal air temperature variation as shown in Fig. 6 (a1) which can be found at the end of the paper. A joint will show opening or closure due to the temperature variation (b1). The sensor and the attachment also show thermoelastic deformation due to the temperature variation (c1).

A daily air temperature deviation from the seasonal variation can be assumed (a2). This will not cause large thermoelastic deformation of rock mass as stated above (b2). On the other hand, the daily variation causes deformation of the sensor and the attachment at the same rate as the seasonal variation (c2).

Assuming an inelastic deformation (b3), the total rock mass deformation (b4) can be obtained as the sum of thermoelastic response of rock mass to the seasonal temperature variation (b1) and the assumed inelastic deformation of rock mass (b3).

Total deformation of the sensor and the attachment (c4) can be calculated as the sum of the thermoelastic response to the seasonal variation (c1) and the daily deviation in temperature (c2).

The observed data (d4) is obtained by subtracting the expansion of sensors and attachments (c4) from the true total rock mass deformation (b4). The joint seems to close when it becomes hotter and open when it becomes warmer by taking the temperature as the x-axis (d4T). However, the errors due to deformation of the sensor and attachment should be removed to know the true deformation of rock mass.

The following equation is used to remove the errors so that the daily data scattering becomes horizontal because the daily scattering is due to the error.

$$U' = U + C_S \Delta T_S$$
$$\Delta T_S = T_S - T_S^0 \qquad (1)$$

where U' is the corrected deformation (d5 and d5T), U is the observed deformation (d4T), T_S is the sensor temperature and T_S^0 is a reference temperature and it is recommended to set T_S^0 around the average sensor temperature. Finally, C_S is the in-situ temperature correction factor for the sensor and attachment, and is calculated based on (d4T). The corrected deformation (d5 and d5T) includes the error due to thermoelastic deformation of the sensor and attachment but the same trend is reconstructed as the true temperature-joint opening plot (b4 and b4T).

Usually, sensors have temperature correction factors. However, a correction based on the correction factor to remove the deformation related to the sensor and the attachment usually does not work because not only the sensor but also the attachment also deform. The deformation of the attachment is unknown and vary from sensor to sensor because attachments are adjusted to various rock surface geometries.

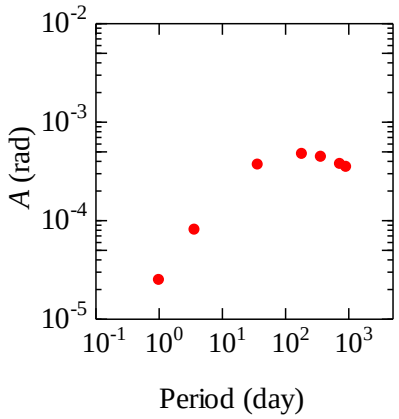

Fig. 4. Result of numerical analyses on the period of temperature variation. *A* is the maximum amplitude of the average inclination of rock block (fracture opening at the top of the cliff divided by *L*).

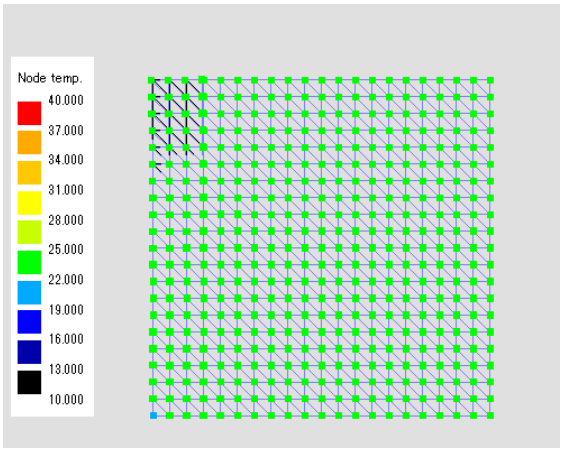

(a) One day period

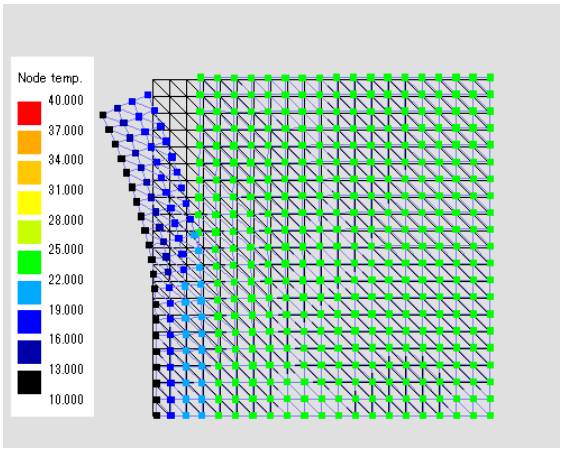

(b) One year period

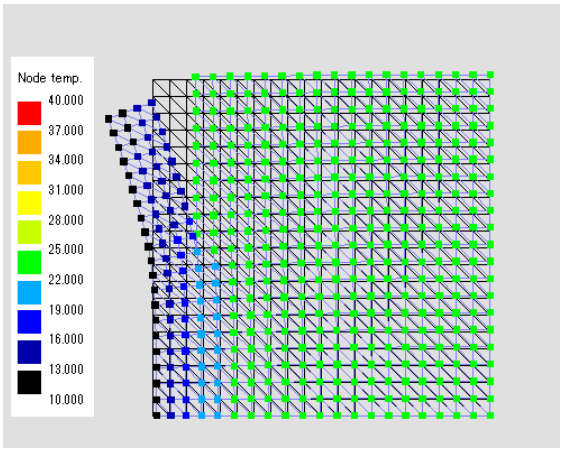

(c) Two year period

Fig. 5. Temperature distribution of the model shown in Fig. 1 (L = 10 (m)) when they show the maximum joint opening. Displacement is magnified by 150 times.

For example, in a basaltic rock cliff along an abandoned national road that is parallel to Toyosaki tunnel in Hakodate, Japan (Toyosaki monitoring site, Fig. 7) fracture opening was monitored with pai-gauge type displacement sensors. The sensor consists of an arch-shaped steel spring plate with strain gauges. The fractures seem to close with temperature rise and open with temperature fall (in the raw data; Fig. 8a). In the temperature-displacement plots, a fracture opening in hot summers is observed (Fig. 9a). The fractures appear to close with increases in temperature and open with falling temperature again, but this may only be an artifact of the thermoelastic deformation of the sensor and the attachment, which is not corrected in the analysis.

The true relationship between fracture deformation and temperature (the red lines in Fig. 9b) can be obtained once the daily thermoelastic deformation is removed from the raw data by Eq. (1). It can be first stated that the joint close when temperature increases and *vice versa* after this correction. This process should generally be applied, although it was consequently found, in this case, that the thermoelastic deformation of the sensors was almost negligible. The rock surface temperature was used for the correction instead of the sensor temperature. The former is generally different from the latter and the difference would affect the accuracy of the reconstruction. The effects seem fortunately not fatal in this case.

4. TECHNIQUE TO ISOLATE THERMOELASTIC DEFORMATION OF ROCK MASS

The relationship between temperature and deformation does not have to be linear, because heat conduction is not instantaneous. However, as long as the relationship is almost linear, the thermal deformation is elastic and it does not indicate instability of the rock block. On the other hand, if the relationship is very non-linear, the rock block deformation will be inelastic and indicates instability.

The thermoelastic deformation of rock mass was isolated by

$$U'' = U' + C_R \Delta T_R$$
$$\Delta T_R = T_R - T_R^0 \qquad (2)$$

where U'' is the corrected deformation, Fig. 6 (d6T), U' is the deformation from which the thermoelastic deformation of sensors and attachments was removed (d5T), T_R is the rock surface temperature and T_R^0 is a reference temperature and it is recommended to set T_R^0 around the average rock surface temperature. Finally, C_R is the in-situ temperature correction factor for the rock mass and is calculated based on (d5T). The correction made the seasonal deformation very small and the inelastic deformation is emphasized (d6T). The assumed inelastic deformation (b3) is almost reconstructed in the time series (d6).

After removing the components of the thermoelastic deformation of rock mass for the Toyosaki case (green lines in Fig. 9c) and replotting the data as a time series (Fig. 8b), significant fracture openings in summer are noted. The cause of the opening was considered to be the growth of the trunk of black locust (*Robinia pseudoacacia*), which intruded into the fracture (Fig. 7b, Maeda et al., 2015).

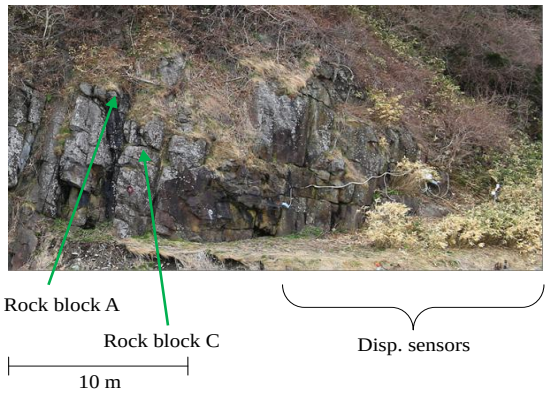

(a) Whole slope

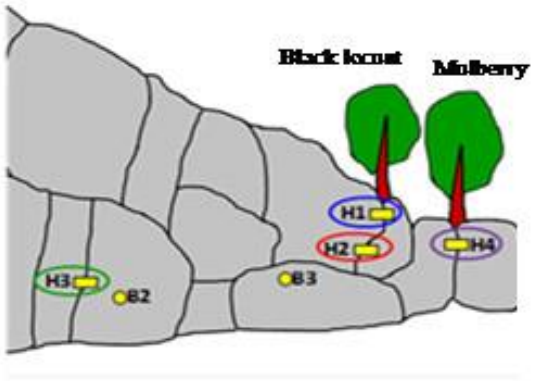

(b) Enlarged schematic figure of displacement sensors

Fig. 7. Toyosaki monitoring site. This figure is not to scale. The height of the cliff is however about 10 m at the left edge of the figure.

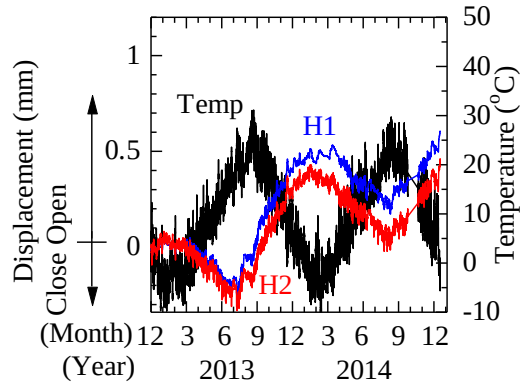

(a) Raw data

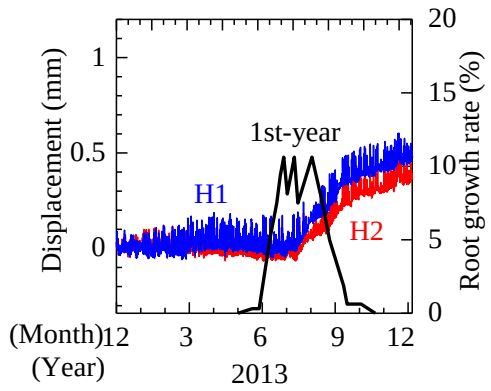

(b) Enlarged plot for only the first year after removing the thermoelastic deformation of sensors and rock mass with the root growth rate of a mulberry (*Morus australis*, Sato, 1985)

Fig. 8. Examples of in-situ monitoring data on time variation of fracture displacement.

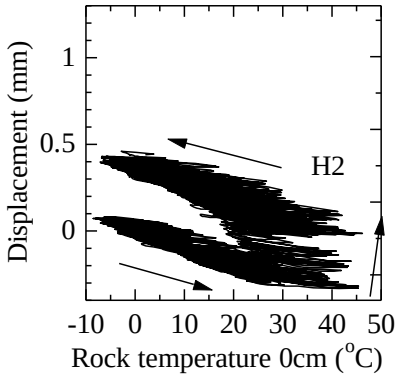

(a) Raw data

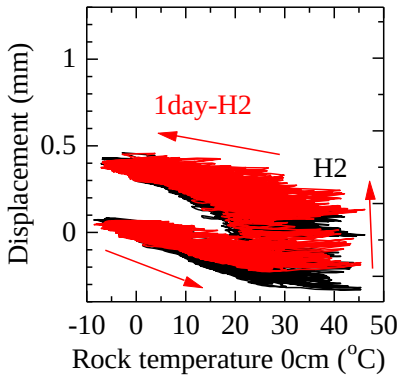

(b) Rock mass deformation after correction for thermal deformation of the sensor (the red line).

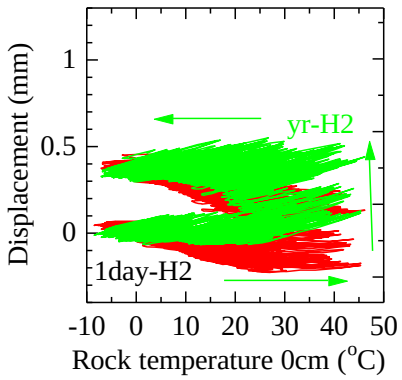

(c) Rock mass deformation after correction for rock mass thermal deformation (the green line).

Fig. 9. An example of fracture opening displacement and rock surface temperature for two years.

5. TECHNIQUE TO MONITOR A VERY UNSTABLE ROCK BLOCK

Techniques for installing a tiltmeter on the top of a very unstable rock block, using a mortar ball and an adjustable seating without any drilling, were proposed and attempted at the Toyosaki monitoring site to resolve problem 1 (Fig. 10; Maeda et al., 2015).

A ladder was used to access the rock block and the data have been recovered using electric cables. A crane with an aerial work platform, and a Wi-Fi data acquisition system with a stable solar power system, could be used to carry out this kind of monitoring for a very unstable rock block at a great height. There is no need to remove the thermoelastic deformation of tiltmeter itself because it does not measure elongation or shrinkage as the pai-gauge type displacement sensors do and there should in principle be no or very little effect of temperature on the output.

The tilt data show variations (Fig. 11) in which thermoelastic deformation and inelastic deformation of rock mass are mixed. Isolating thermoelastic deformation of rock mass by using the technique described in chapter 4 and plotting the data as a time series, it was found that the tilt of block A was thermoelastic deformation of rock mass. On the other hand, a non-thermoelastic deformations after the 250th day (i.e., at the end of September) were seen for block C (Fig. 12). The non-thermoelastic deformations were interpreted as inelastic deformation of the rock mass triggered by the heavy precipitation during the typhoons in the late summer (around 240th day).

(a) Installation (b) Zoomed up image

Fig. 10. Tiltmeter installation on the top of the very unstable rock block (rock block A).

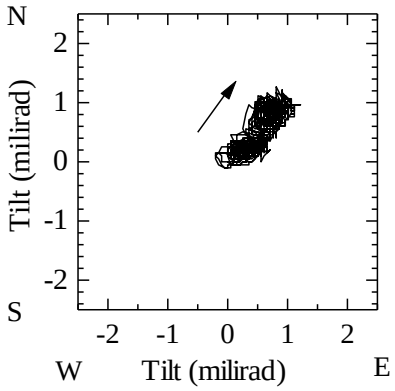

(a) Rock block A

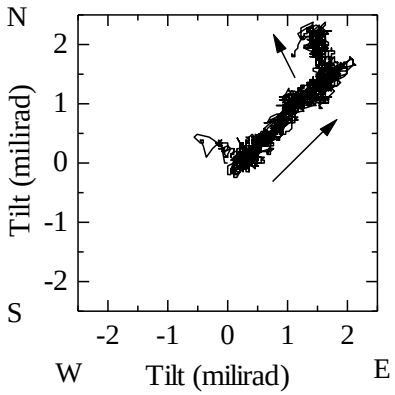

(b) Rock block C

Fig. 11. Examples of observed inclination vectors.

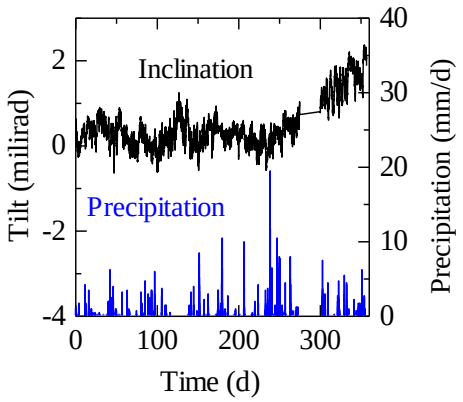

(a) Rock block C in North direction

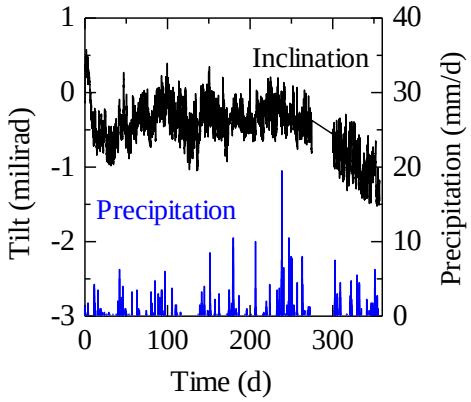

(b) Rock block C in West direction

Fig. 12. Time series of precipitation data and tilt data after the thermoelastic deformation of rock mass was removed. Time in day is from Dec. 14, 2013.

6. CONCLUDING REMARKS

The basic mechanisms of thermoelastic deformation of a beam-like rock block formed by fracturing were explained. Easy techniques to separate the thermoelastic deformation of sensors and attachments from observed rock mass deformation data, to isolate the thermoelastic deformation of rock mass and to monitor the tilt of a very unstable rock block were described.

The techniques described in this paper were developed to solve the problems that interfere with the advancement of understanding of the rock mechanics underlying unstable rock blocks. The techniques may not appear to be particularly novel, sophisticated or attractive, but they can be used for planar or wedge failures or for more complex instabilities developed by more than one joint set. The authors are convinced that they will contribute to breakthroughs in solving the listed problems. The techniques are inexpensive and just require shifts in thinking.

The authors would be greatly appreciative if readers could apply some of the techniques, which may also work well in combination with our new methods of predicting failure time (Mufundirwa et al., 2010) and failure volume (Fujii et al., 2014) according to displacement rate. We will eagerly await feedback.

ACKNOWLEDGMENT

The authors express their deepest gratitude to the Hokkaido Road Management Engineering Center (RMEC) for financially supporting this study.

REFERENCES

1. Fujii, Y., A. Mufundirwa, J. Kodama. and D. Fukuda. 2014. Prediction of Time and Volume of Rock Failure by Slope Method, *Proceedings of the 3rd. International Conference on Advances in Mining and Tunneling (ICAMT 2014), Vung Tau, Vietnam, Oct. 22, 2014*, 285-289.
2. Keppetipola, S.S.S.S.M., Y. Fujii and N. Kodama. 2013. Mechanisms of Falling Rock Formation at Steep Slope due to Temperature Perturbation. *In Proceedings of 47th US Rock Mechanics/Geomechanics Symposium, San Francisco,USA, 23-26 June 2013*, Paper No. 13-237.
3. Maeda, S., K, Togashi, T. Sugawara, Y. Fujii, N. Kodama, N. Miyashita. 2015 in Japanese. Long-term Monitoring and Numerical Analysis of Thermal Deformation for a Steep Cliff in Cold Region, *In Proceedings of Spring Meeting, Hokkaido Branch, MMIJ, Sapporo, Japan, June 13, 2015*, 17-18.
4. Mufundirwa, A., Y. Fujii and J. Kodama. 2010. A New Practical Method for Prediction of Geomechanical Failure-time, *International Journal of Rock Mechanics and Mining Sciences*, 47:7,1079-1090
5. Negishi, M. and I. Nakajima. 1993 in Japanese. Mechanism of Toppling of Long Columnar in Sounkyo Welded Tuff — Study on Slope Failure in Cold Region (2nd Report)—. *Journal of the Japan Society of Engineering Geology*, 34:2,1-11.Fig. 10. Time series of inclination data after thermal deformation was removed with precipitation data. Time in day is from Dec. 14, 2013.

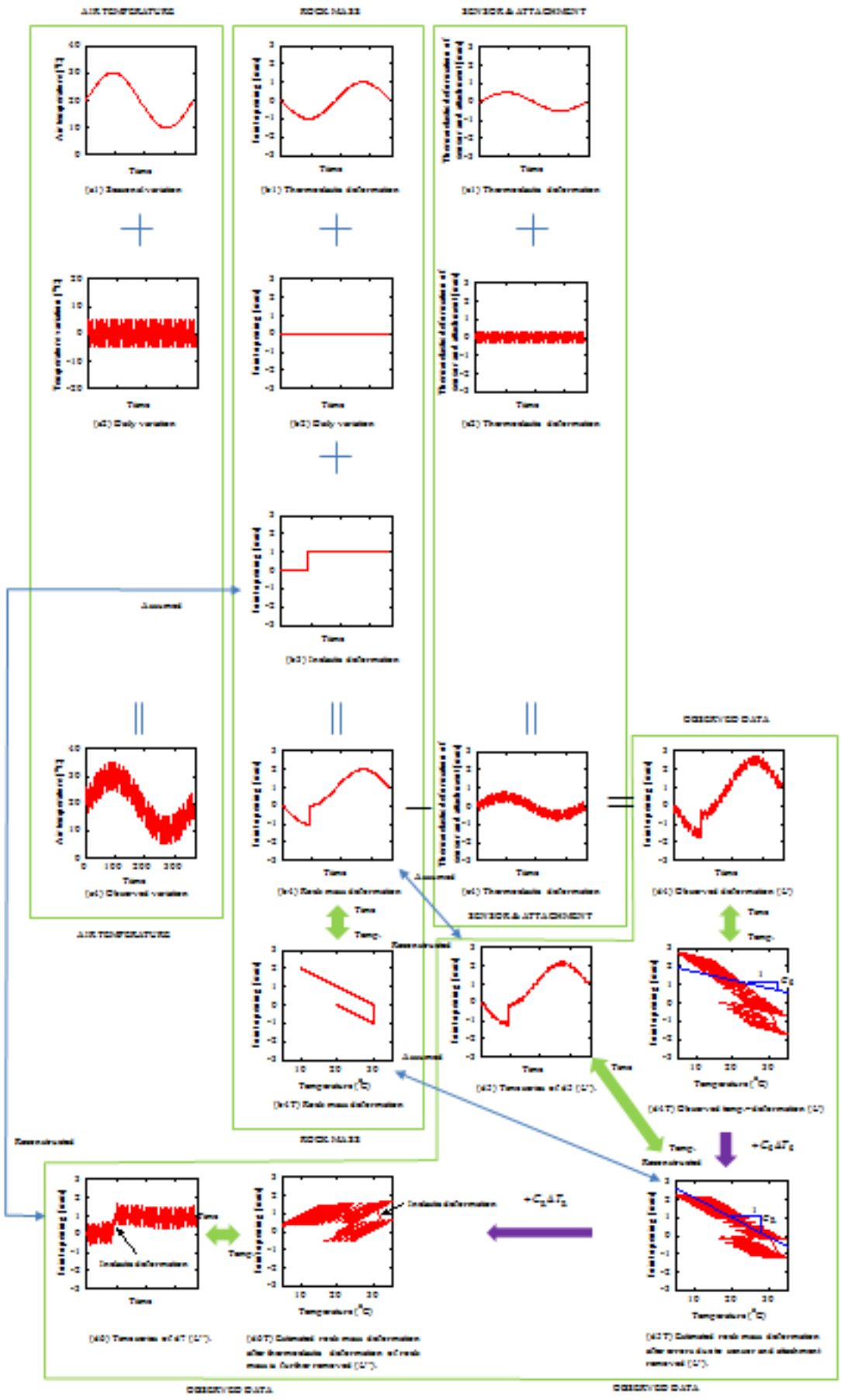

Fig. 6 (whole) Graphical explanations of the effects of temperature on observed data and reconstruction of rock mass deformation. Enlarged figures follows.

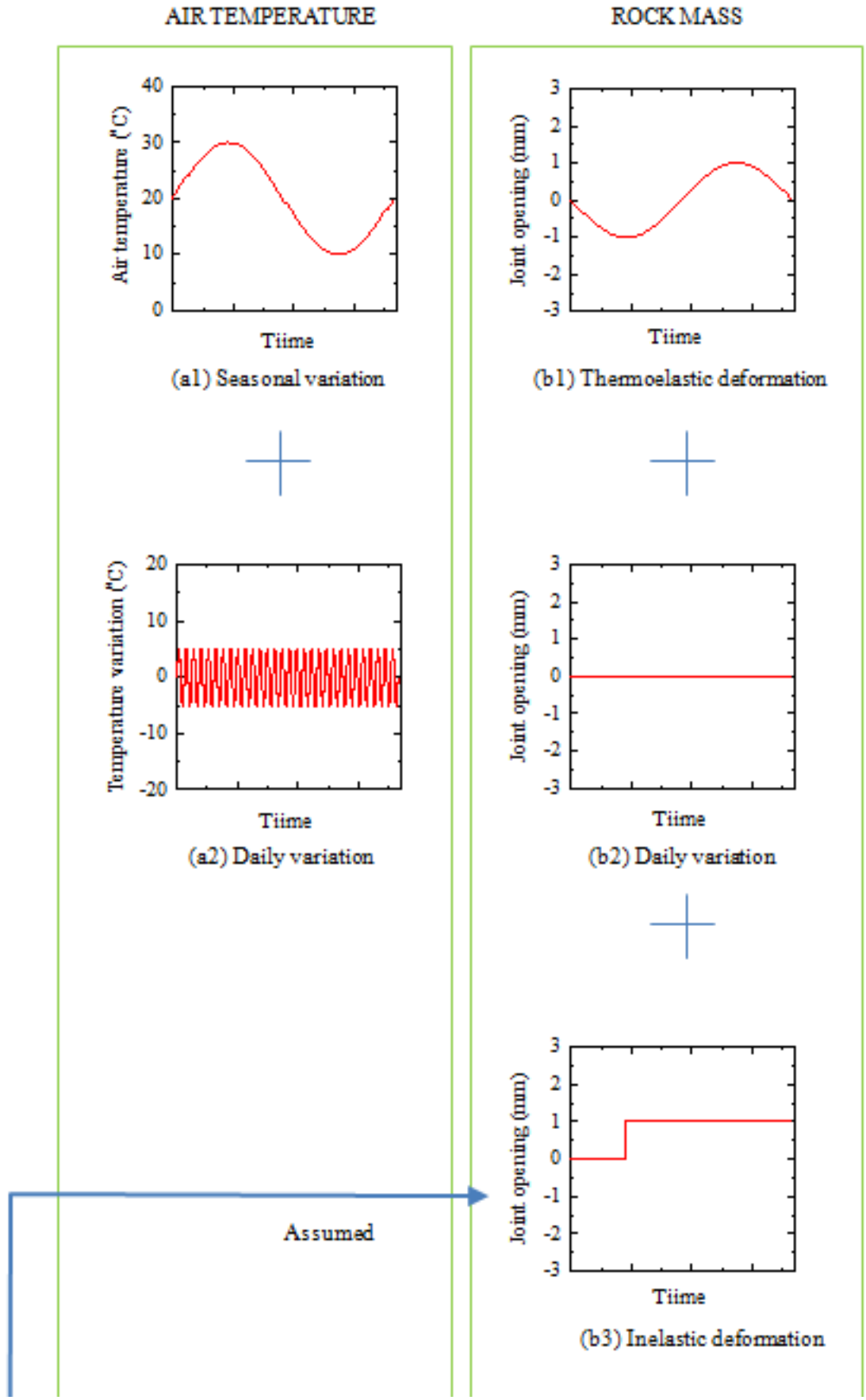

Fig. 6 The upper left part.

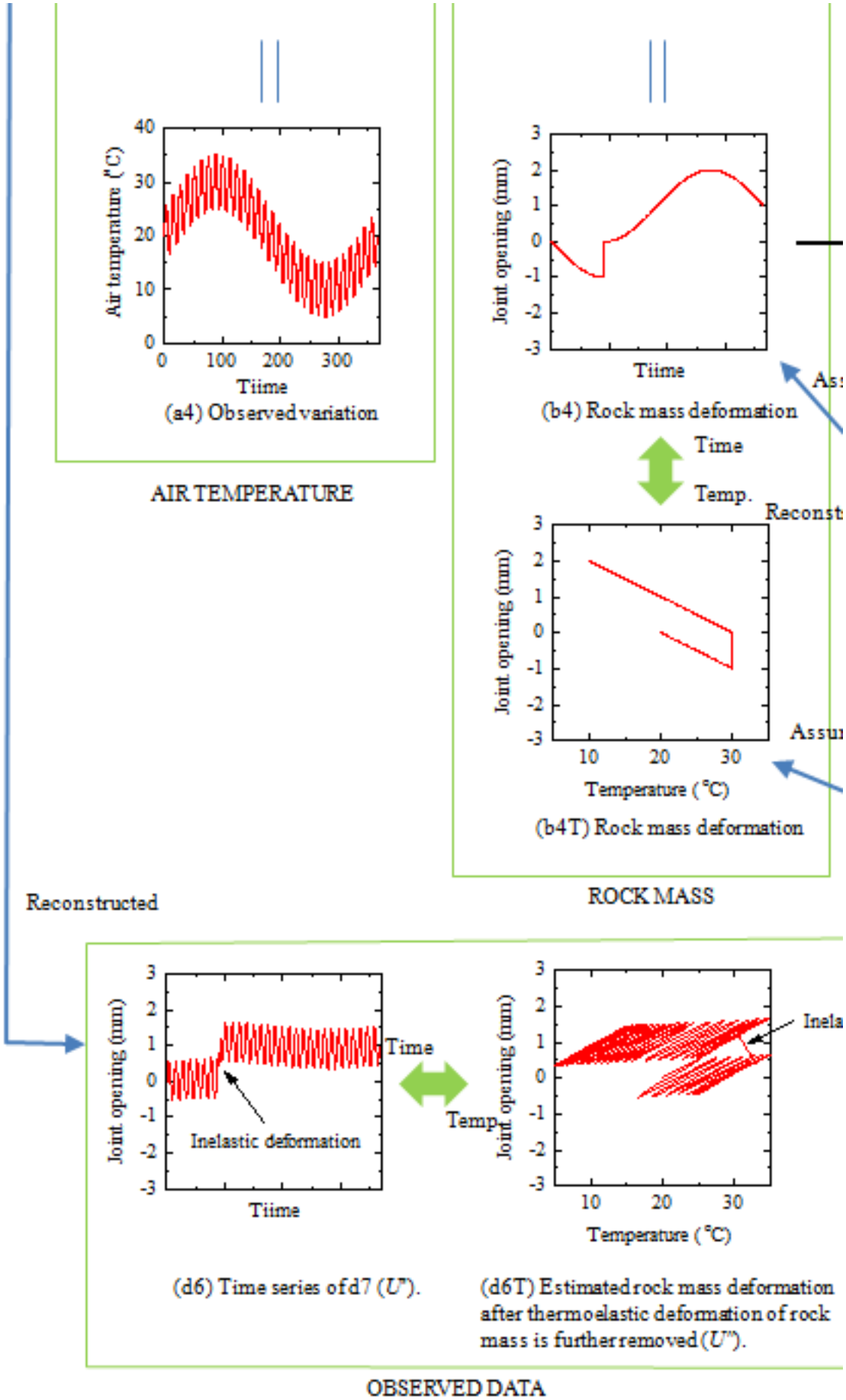

Fig. 6 The lower left part.

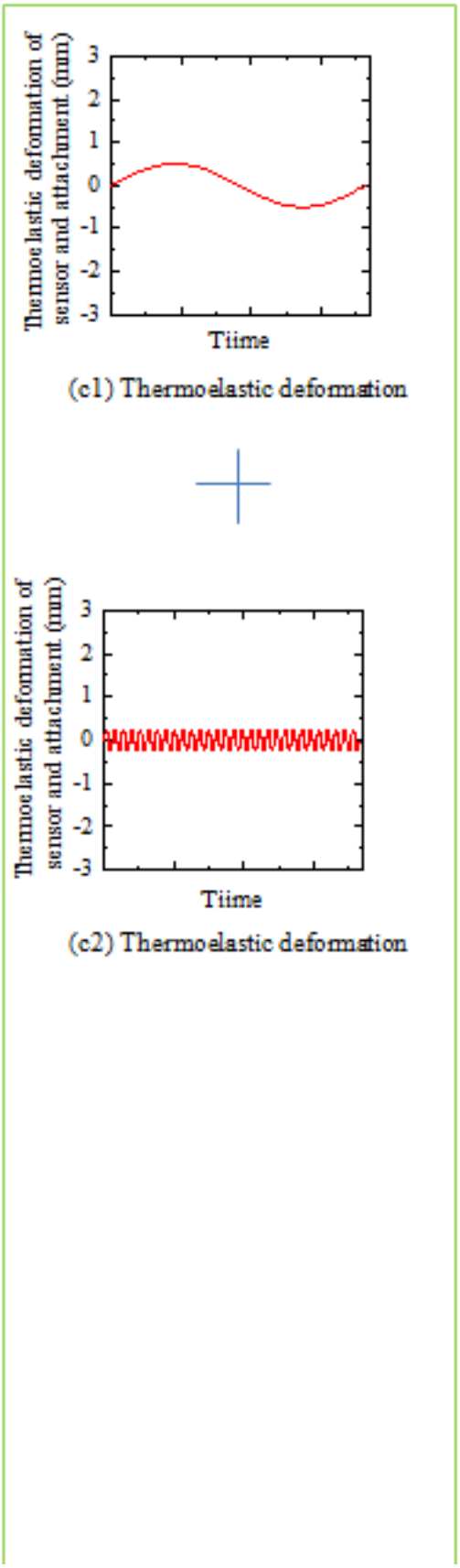

Fig. 6 The upper right part.

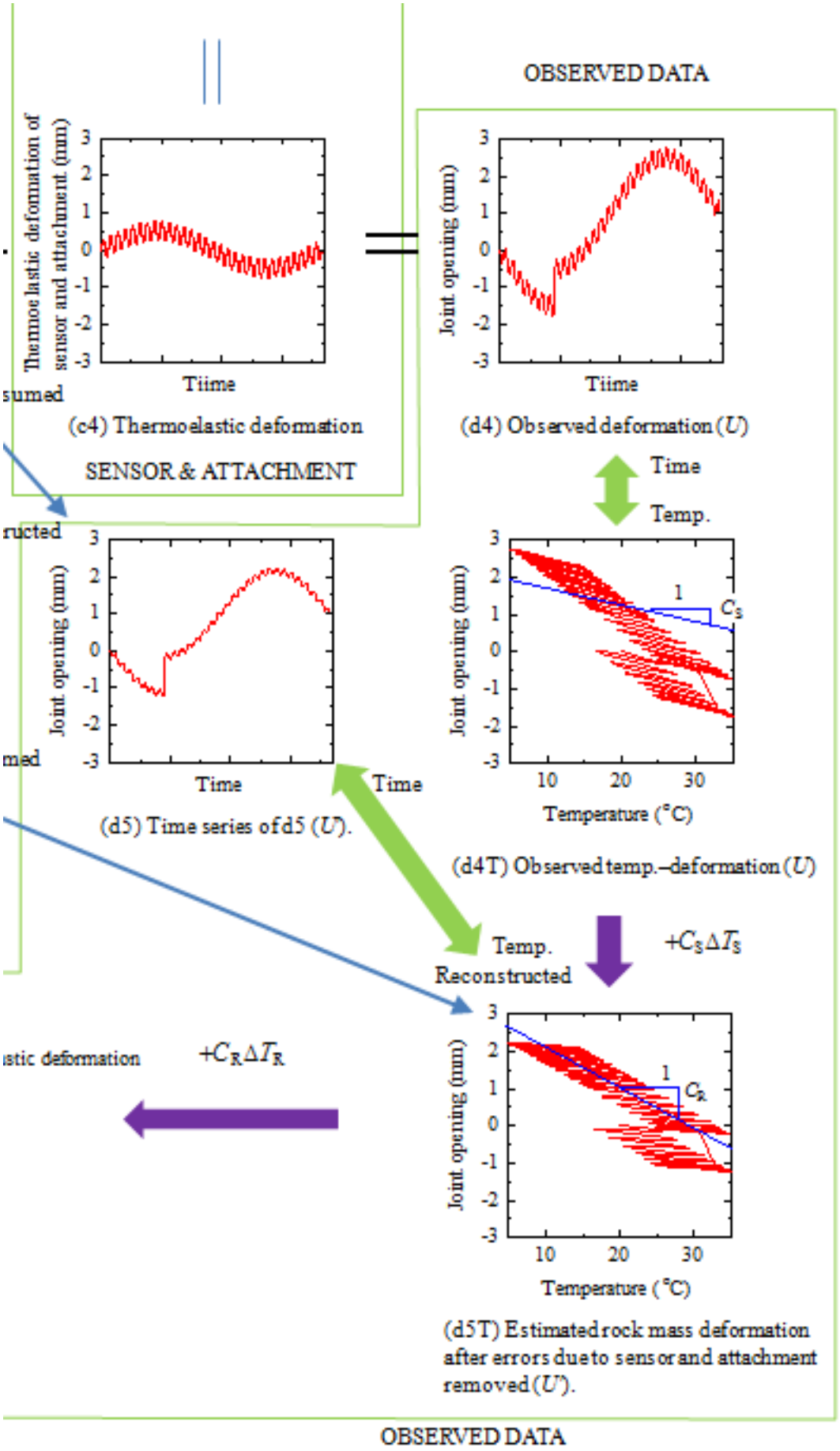

Fig. 6 The lower right part.